Surface Chemistry

DOI: 10.1002/anie.201201083

Reactivity of Surfaces Determined by Local Electrochemical Triggering: A Bromo-Terminated Self-Assembled Monolayer**

*Sandra Nunige, Renaud Cornut, Hassan Hazimeh, Fanny Hauquier, Christine Lefrou, Catherine Combellas, and Frédéric Kanoufi**

The assessment of chemical reactivity of surface-bound targets is of fundamental importance in many fields of research, because the reactivity cannot be directly deduced from similar reactions performed in solution. A key issue in biological systems where target-search strategies must be optimized[1] or in the building of molecular functional interfaces. For example, the bottom-up strategy uses mild and highly selective coupling reactions at self-assembled monolayers (SAMs). A large number of such block-building approaches proceeds through metal-complex-catalyzed redox reactions such as in "click" chemistry,[2] Sonogashira couplings,[3] or atom-transfer radical polymerization (ATRP).[4] Scanning electrochemical microscopy (SECM) is the most appropriate tool to investigate the chemical reactivity of surfaces.[5] From its local inspection, SECM allows a simple combinatorial analysis of surface reaction mechanisms.[6] The surface interrogation mode, based on transient feedback current measured at the tip (SI-SECM),[7] is a priori the most advanced strategy as it allows the in situ detection of sub-monolayer transformations. Herein, in addition to the SI-SECM mode, we have followed a lithographic approach, which is likely more robust since it is not based on electrochemical measurements alone. This approach relies on using a tip as a microsource of a chemical reagent to write patterns on the surface. Such (electro)chemically induced patterning strategies offer wide chemical diversity at interfaces.[5] Recently this strategy was proposed as an insightful quantitative access to the local chemical reactivity of surfaces, based on the ex situ reading of the time evolution of patterns written on a surface.[8,9] This strategy is developed for SECM and must apply to other patterning tools such as the scanning ion conductance microscope (SICM).[10]

Here, we show the potential of this patterning strategy by comparing it to the SI-SECM mode in the case of the reductive transformation of bromo-terminated SAMs (Br-SAMs shown in Scheme 1) immobilized onto insulating Si/SiO_2 or glass surfaces. The interest in the intrinsic redox reactivity of Br-terminated SAMs originates from their derivatization potential by "click" chemistry[11,12] or by ATRP growth of polymer brushes.[4,13] Moreover, both reactions have been adapted to surface patterning by SECM.[12,14] We focus on the evaluation of the reactivity of Br-SAMs toward a tip-electrogenerated reducer, Red, the anion radicals of 2,2′-bipyridine (bpy) or of nitrobenzene (nbz). Basically, with bpy the reaction at the substrate surface is given by Equations (1) and (2) where the kinetically

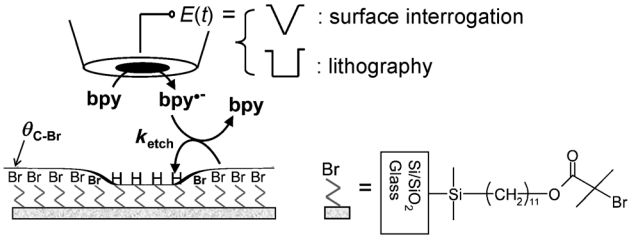

Scheme 1. Description of local electrochemical triggering of a Br-SAM reactivity by transient feedback or patterning experiments.

$$bpy^{\bullet -} + R{-}Br \xrightarrow{k_{etch}} R^{\bullet} + Br^{-} + bpy \quad (1)$$

$$bpy^{\bullet -} + R^{\bullet} \rightarrow bpy + R^{-} \xrightarrow{SH} RH \quad (2)$$

limiting step is the bimolecular heterogeneous first electron transfer (1) with a rate constant, k_{etch}, corresponding to the reductive breaking of the C–Br bond.

This combination of reactants leads to a fast surface reaction in the limit of control by the lateral diffusion of the etchant $bpy^{\bullet -}$, in accordance with mechanistic studies of parent solubilized Br moieties.[15] As shown in the following, tuning the chemical instability of $bpy^{\bullet -}$ allows to expand the accessible range of surface reaction kinetics.

[*] S. Nunige, Dr. H. Hazimeh, Dr. F. Hauquier, Dr. C. Combellas, Dr. F. Kanoufi
Physico-Chimie des Electrolytes, des Colloides et Sciences Analytiques, ESPCI ParisTech, CNRS UMR 7195
10 rue Vauquelin, 75231 Paris Cedex 05 (France)
E-mail: frederic.kanoufi@espci.fr
Dr. R. Cornut,[+] Prof. Dr. C. Lefrou
Laboratoire d'Electrochimie et de Physico-chimie des Matériaux et des Interfaces
UMR 5279 CNRS-Grenoble-INP-UJF
1130 rue de la piscine, B.P. 75, Domaine Universitaire
38402 Saint Martin d'Hères Cedex, (France)
[+] Current address:
CEA-Saclay, Laboratoire de Chimie de Surface et Interface
91191 Gif-sur-Yvette Cedex (France)

[**] The "Agence Nationale de la Recherche", ANR, is gratefully acknowledged for its financial support via the ANR-06-BLAN-0368 project. R.C. thanks the ANR for partial financing via the ANR-PDOC20011-Copel. H.H. thanks the ESPCI Paris Tech for its financial support.

Supporting information including experimental details, modeling and electrochemical procedures at the surface and in solution and chemical amplification for this article is available on the WWW under http://dx.doi.org/10.1002/anie.201201083.

From the two different types of experiments, presented in Scheme 1, which are tested to interrogate the surface transformation, that is, by transient electrochemical SECM and writing readable patterns on Br-SAMs, the Br-SAM coverage and its reactivity are obtained through modeling of the irreversible transformation of a monolayer of active material (detailed in the Supporting Information). Briefly, in addition to Equation (1) the chemical instability of the etchant $bpy^{\bullet-}$ is taken into account in Equation (3) (not shown in Scheme 1 for simplicity):

$$bpy^{\bullet-} \xrightarrow{k_c} pdct \qquad (3)$$

Different dimensionless parameters are used to explore the variety of situations: the dimensionless surface coverage γ ($\gamma = \Gamma^0/C^0 a$, where Γ^0 is the initial Br-SAM surface concentration, a is the tip radius, and C^0 is the redox probe concentration), the dimensionless surface transformation constant ($\lambda_{etch} = k_{etch} C^0 a^2/D$, where D is the redox probe diffusion coefficient) and the dimensionless solution reaction constant ($\lambda_c = k_c a^2/D$). Another dimensionless parameter is also interesting as it compares readily with usual monomolecular heterogeneous electron transfer (ET) in feedback experiments: $\Lambda = \lambda_{etch}\gamma = k_{etch}\Gamma^0 a/D$ ($k_{etch}\Gamma^0$ in $cm\,s^{-1}$). As such, the model is used to describe the transformation of immobilized RBr both in the SI-SECM, through computation of the tip current, and in the lithographic mode, through calculation of the pattern growth.

As a preliminary step, in every case, the rate k_c is estimated from the digital simulation of the cyclic voltammetric (CV) response at the SECM tip at infinite distance from the SAM surface. The observation of the oxidation peak of $bpy^{\bullet-}$ on the reverse scan at a potential scan rate of $1\,V\,s^{-1}$ (Figure 1a) ensures that $bpy^{\bullet-}$ is engaged in an irreversible chemical transformation, with a λ_c value equal to 1 ± 0.1, that corresponds to an apparent first-order rate constant, k_c, equal to $(6 \pm 0.5)\,s^{-1}$ (considering $D = 10^{-5}\,cm^2\,s^{-1}$). According to a first-order mechanism, the same rate constant is found, $k_c = (5 \pm 2)\,s^{-1}$, with mediator (bpy) concentrations ranging from 0.2 to 5.3 mM. However, in the case of a highly concentrated solution, 50 mM, a lower apparent first-order rate constant of $(0.25 \pm 0.05)\,s^{-1}$ is found. This shows that the mechanism for Equation (3) is not of pure first order, probably because of the complex processes responsible for the unstability of the electrogenerated radical anion species. The radical anion may react with many compounds present as traces such as water, O_2, or its reduction products, such as $HO^{\bullet}$. Even if the latter are easily generated at Pt electrodes,[16] from CV inspection O_2 was always at trace level compared to Red under our controlled inert atmosphere (see the Supporting Information). Moreover, $nbz^{\bullet-}$ is stable which disfavors the action of $HO^{\bullet}$ and suggests the prominent role of water traces in k_c.

In a next step, the SI-SECM mode has been used to estimate both the transformation rate, k_{etch}, and the surface concentration of the Br-SAM, Γ^0, from indirect inspection by CV. These quantities are obtained from comparison of the experimental voltammograms (Figure SI.2 in the Supporting Information) recorded for the reduction of bpy at a tip held above a Br-SAM or above the same layer once it had been etched by $bpy^{\bullet-}$ at the tip for 100 s. The experimental conditions (tip–substrate distance, scan rate, and etching time) must be optimized to get the response of the SAM. This was already discussed[7] and a more general optimization of the conditions and sensitivity of the method is behind the scope of the present article. Here for example, the time used for the potential cycle is long enough for $bpy^{\bullet-}$, given its instability, to travel back and forth from the tip to the SAM. It then yields an electrochemical response at the Br-SAM which is higher than at the etched SAM. The difference between both curves reflects the feedback current difference because of the regeneration of bpy from the etching of the Br-SAM [Eqs. (1 + 2)]. Figure 1b shows the experimental feedback current difference recorded for this process at $0.1\,V\,s^{-1}$. As already pointed out,[7] the appropriate modeling of such experiments is delicate as it depends on different experimental parameters. Here, a good fit can be obtained for different (k_{etch}, Γ^0) couples (Figure SI.3 in the Supporting Information). The appropriate choice relies, as for desorption processes,[7] on the independent estimate of the surface concentration Γ^0. It is based on the integration of the feedback current used to etch the Br-SAM during cyclic voltammetry (CV; 2.8 nC), which is compared to the dimension of the transformed domain during CV. The latter is obtained, as described later, from ex situ observation on the surface of a pattern three times larger than the tip. This corresponds to an exchange of $0.6\,nmol\,cm^{-2}$ of electron or, for a $2e^-$ process, to a Br-SAM surface concentration of $\Gamma^0 = 0.3\,nmol\,cm^{-2}$, in agreement with the maximum surface coverage by a silane monolayer

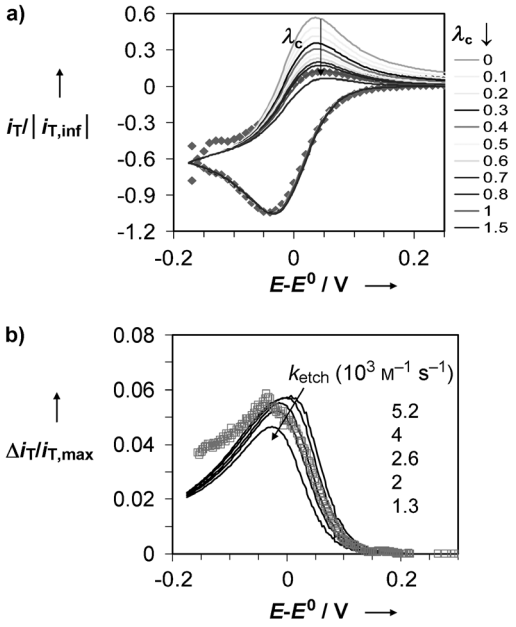

Figure 1. Cyclic voltammetry of 5.3 mM bpy and 0.1 M NBu_4BF_4 in dimethylformamide (DMF) solution at a Pt tip of a radius $a = 12.5\,\mu m$. a) $\nu = 1\,V\,s^{-1}$, tip held at $d = 150\,\mu m$ from the Br-SAM (infinite d), experimental points (◆) with theoretical responses for different λ_c. b) Surface interrogation of the reducibility of the Br-SAM at $\nu = 0.1\,V\,s^{-1}$, tip held at $d/a = 0.47$. Feedback current difference (□) compared to calculated responses with $k_c = 6\,s^{-1}$ and $\Gamma^0 = 0.3\,nmol\,cm^{-2}$ for different k_{etch}.

(0.5 nmol cm^{-2}).[17] Considering the etchant instability obtained from CV far from the substrate ($k_c = 6\ s^{-1}$) and $\Gamma^0 = 0.3$ nmol cm^{-2}, a reasonable fit (Figure 1b) of the feedback CV transient response is obtained for a surface reaction rate $k_{etch} = (2.5 \pm 0.5) \times 10^3\ M^{-1}\ s^{-1}$. This shows that the SI-SECM mode is not limited to surface concentration quantification, and can also be useful to determine kinetic constants through appropriate numerical simulation of the curves. It is particularly appealing for the access to fast reaction rates provided by the use of fast potential scan rates combined with small tip–substrate distances.

The SI-SECM strategy was then compared to the lithographic mode of the SECM for kinetic determination. The theoretical results for this mode are presented in Figure 2a–c. Figure 2a shows a typical evolution of the pattern radius, $R = r/a$, with the dimensionless reaction time, $\tau = tD/a^2$. As expected, the patterns grow faster when the surface coverage γ decreases. To better apprehend the writing kinetics, it is easier to follow the evolution of $\tau_{(R=5)}$, the characteristic time required to draw a pattern of radius $R = 5$ (dashed line in Figure 2a). Figure 2b shows this characteristic time $\tau_{(R=5)}$ as a function of the surface coverage γ, for different surface transformation constants. Limiting situations are observed for Λ values. At high Λ, the etching is diffusion controlled and only γ and λ_c influence the pattern evolution (see the Supporting Information). Then, γ and λ_c may be determined but not λ_{etch}. The condition for this limiting case (the vertical asymptotes in Figure 2c) does not depend on γ, but on λ_c: the higher λ_c, the higher the maximal λ_{etch} that can be determined (see the Supporting Information). This is useful to improve the range of accessible λ_{etch} by changing λ_c: the decrease of the etchant lifetime allows the time characteristic for surface transformation to be governed by the interfacial reaction kinetics, not by the characteristic diffusion time. Another limit case is encountered as revealed by the horizontal asymptotes in Figure 2c. At low Λ (low λ_{etch}), the process is governed by the surface transformation kinetics: only λ_{etch} and λ_c influence the pattern evolution, and γ cannot be determined.

This shows that there is a limited range of experimental conditions where the determination of both λ_{etch} and γ is possible. For a given material, it is possible to reach the appropriate experimental conditions by changing the tip radius or Γ^0: for example, from the high Λ regime, higher rates k_{etch} are accessible with smaller tips and smaller Γ^0. Alternatively, the value of k_c can be tuned to determine high k_{etch} values. As discussed elsewhere[9] the tip–substrate distance, d, and the dimension of the insulating sheath of the tip (RG) have less contrasted incidence on the pattern evolution and are not discussed in this work. Particular care should be taken at high k_c values which yield small patterns less dependent on RG but require sufficient small d values for allowing the etchant to reach and react with the SAM.

In the following we discuss the application of this lithographic strategy for Br-SAM reactivity assessment. Patterns were written on the Br-SAM-modified glass for different etching times with a static SECM tip of 12.5 or 25 μm radius in different bpy solutions ($C^0 = 0.2$, 0.4, 2, and 50 mM). As already proposed, the patterns are chemically amplified by the growth of polymer brushes and then read from condensation figures (Figure 2d).[14] The patterning results are presented in Figure 2e. At the highest C^0, λ_c is 0.04 according to preliminary CV experiments, and the pattern evolution fits the expectations for the case of diffusion controlled etching (dashed lines in Figure 2e). The determination of λ_{etch} is thus not possible in this case, and only γ can be determined. The fit with a RBr surface coverage Γ^0 of 0.3 nmol cm^{-2} is good for both $a = 25$ and 12.5 μm. A decrease in the redox probe

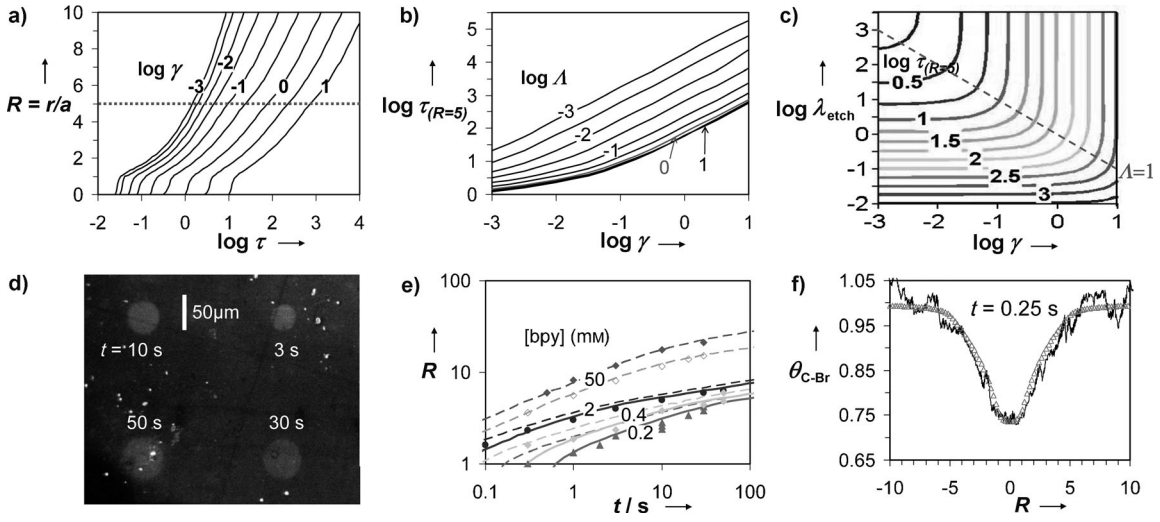

Figure 2. Surface reactivity from SECM lithography. a–c) Theoretical pattern growth, $\lambda_c = 0.1$. Influence of the surface coverage on the pattern radius R growth with the dimensionless time $\tau = tD/a^2$ (a) and influence of the etching time needed to write a $R = 5$ pattern with the reactant concentrations Γ^0 and C^0 and the reaction rate $\Lambda = \lambda_{etch}\gamma$ (b) and λ_{etch} (c). d–f) Writing with a tip-generating Red on a Br-SAM. d) Patterns read from condensation figures, Ox = bpy (0.4 mM). e) Pattern growth for Ox = bpy: (◇) $a = 25$ μm, otherwise $a = 12.5$ μm, RG = 5, L = 0.47; fitted with $k_c = 0.25\ s^{-1}$ for $C^0 = 50$ mM (◆,◇) and 5 s^{-1} otherwise; $\Gamma^0 = 0.3$ nmol cm^{-2}, for $C^0 =$ ● 2, ◆ 0.4, ▲ 0.2 mM. Dashed lines: diffusion control. Solid lines: $k_{etch} = 1.3 \times 10^4\ M^{-1}\ s^{-1}$. f) Ox = nbz (50 mM), $a = 25$ μm. Experimental Br-SAM surface coverage, $\theta_{C\text{-}Br}$, within a pattern (△) fitted with $k_{etch} = 1\ M^{-1}\ s^{-1}$ and $k_c = 0$.

concentration, C^0, results in a higher value of λ_c ($\lambda_c = 0.7$, as observed in CV experiments), so that the patterns become smaller relative to the diffusion-limited patterns. The experiments are thus not conducted in the large λ_{etch} regime any more, and λ_{etch} can be evaluated. Using the γ value determined at high $C°$, the pattern evolution is compared to theory and a k_{etch} value of $(1.3 \pm 0.2) \times 10^4\,M^{-1}s^{-1}$ is obtained, in agreement with that obtained from SI-SECM.

The agreement between both analyses is convincing to propose lithographic experiments to assess the kinetics of irreversible surface transformation. The C–Br bond activation in Br-SAMs proceeds with an ET rate which is lower than that of ferrocene-bound (Fc-bound) moieties.[18–20] It reflects an inner-sphere (dissociative) ET, which likely takes place at the Br-SAM, as observed for the solubilized parent Br molecule (see the Supporting Information). Moreover, as for other immobilized systems, the solubilized parent reacts more rapidly than in the SAM (400 times here, see the Supporting Information).

In principle by increasing the etchant instability, transformation rates of around $10^7\,M^{-1}s^{-1}$ are accessible by the lithographic mode. Slower transformation rates are also easily amenable while they cannot be detected by the SI-SECM mode. Slower transformations of Br-SAMs were obtained by lowering the driving force of Equation (1) and generating at the tip the nitrobenzene anion radical, $nbz^{\bullet-}$ ($E^0 = -1.08$ V vs. saturated calomel electrode, SCE). At short etching times, sub-monolayer transformation is detected. The amount of unreacted C–Br within a pattern, θ_{C-Br} (Figure 2 f), was attested from their engagement in growth of polymer brushes by ATRP and shown by local ellipsometric measurement (see the Supporting Information).[14] The comparison of the pattern to theory (Figure 2 f) yields $k_{etch} = (12 \pm 2)\,M^{-1}s^{-1}$. For a linear activation-driving force variation, the C–Br reductive transformation is associated to a transfer coefficient $\alpha = RT\,d\ln(k_{etch})/F dE^0 = 0.18$, in favor to a large reorganization, as in bond-dissociative ET.[15]

In summary, we have shown that the chemical reactivity of a bromo-terminated SAM immobilized on an insulating substrate can be quantified from the time evolution of patterns formed during the local reduction of the SAM. The transformed material can be quantified with sub-monolayer resolution and at transformation rates ranging from 10 to $10^4\,M^{-1}s^{-1}$ (equivalent heterogeneous rates are 3×10^{-6} to $3 \times 10^{-3}\,cm\,s^{-1}$). The potential of this lithographic strategy for SAM reactivity is described from theoretical and experimental points of view and compared to surface interrogation by electrochemical microscopy. Both show concordant results, while the range of applications is higher with the lithographic mode. The approach is obviously not restricted to the specific C–Br bond cleavage activation and can be adapted to block-building reactions from surfaces. For example, the present model allows interpreting the electrochemically assisted surface patterning by click chemistry[12] with an apparent click reaction rate, $k_{click} = 0.02\,s^{-1}$. This illustrates that the lithographic mode of the SECM is a versatile tool to understand the reactivity and selectivity of any surface-bound chemical target. It is even not restricted to redox reagents owing to the chemical diversity that can be generated by SECM electrochemical activation or by a SICM micropipette delivering system. It should be possible to scrutinize a wide range of organic,[16,21,22] organometallic,[23] or inorganic[24] chemical reactions, which is a fundamental issue to assist in the rational selection of conditions for surface or material synthesis.

Received: February 8, 2012
Published online: April 12, 2012

Keywords: kinetics · electrochemistry · self-assembly · surface chemistry

[1] O. Bénichou, C. Loverdo, M. Moreau, R. Voituriez, *Phys. Chem. Chem. Phys.* **2008**, *10*, 7059.
[2] V. V. Rostovtsev, L. G. Green, V. V. Fokin, K. B. Sharpless, *Angew. Chem.* **2002**, *114*, 2708; *Angew. Chem. Int. Ed.* **2002**, *41*, 2596; C. W. Tornøe, C. Christensen, M. Meldal, *J. Org. Chem.* **2002**, *67*, 3057.
[3] M. Müri, B. Gotsmann, Y. Leroux, M. Trouwborst, E. Lörtscher, H. Riel, M. Mayor, *Adv. Funct. Mater.* **2011**, *21*, 3706.
[4] a) K. Matyjaszewski, P. J. Miller, N. Shukla, B. Immaraporn, A. Gelman, B. B. Luokala, T. M. Siclovan, G. Kickelbick, T. Vallant, H. Hoffmann, T. Pakula, *Macromolecules* **1999**, *32*, 8716; b) R. Barbey, L. Lavanant, D. Paripovic, N. Schuwer, C. Sugnaux, S. Tugulu, H.-A. Klok, *Chem. Rev.* **2009**, *109*, 5437.
[5] G. Wittstock, M. Burchardt, S. E. Pust, Y. Shen, C. Zhao, *Angew. Chem.* **2007**, *119*, 1604; *Angew. Chem. Int. Ed.* **2007**, *46*, 1584.
[6] J. L. Fernández, D. A. Walsh, A. J. Bard, *J. Am. Chem. Soc.* **2005**, *127*, 357.
[7] a) J. Rodríguez-López, M. A. Alpuche-Avilés, A. J. Bard, *J. Am. Chem. Soc.* **2008**, *130*, 16985; b) Q. Wang, J. Rodriguez-López, M. A. Alpuche-Avilés, A. J. Bard, *J. Am. Chem. Soc.* **2009**, *131*, 17046; c) J. Rodriguez-López, M. A. Alpuche-Avilés, A. J. Bard, *J. Am. Chem. Soc.* **2010**, *132*, 5121.
[8] C.-A. McGeouch, M. A. Edwards, M. M. Mbogoro, C. Parkinson, P. R. Unwin, *Anal. Chem.* **2010**, *82*, 9322.
[9] H. Hazimeh, S. Nunige, R. Cornut, C. Lefrou, C. Combellas, F. Kanoufi, *Anal. Chem.* **2011**, *83*, 6106.
[10] C. Laslau, D. E. Williams, B. Kannan, J. Travas-Seidic, *Adv. Funct. Mater.* **2011**, *21*, 4607.
[11] G. E. Fryxell, P. C. Rieke, L. L. Wood, M. H. Engelhard, R. E. Williford, G. L. Graff, A. A. Champbell, R. J. Wiacek, L. Lee, A. Halverson, *Langmuir* **1996**, *12*, 5064.
[12] S.-Y. Ku, K.-T. Wong, A. J. Bard, *J. Am. Chem. Soc.* **2008**, *130*, 2392.
[13] a) J. Qiu, K. Matyjaszewski, L. Thouin, C. Amatore, *Macromol. Chem. Phys.* **2000**, *201*, 1625; b) A. J. D. Magenau, N. C. Strandwitz, A. Gennaro, K. Matyjaszewski, *Science* **2011**, *332*, 81.
[14] C. Slim, Y. Tran, M. M. Chehimi, N. Garraud, J.-P. Roger, C. Combellas, F. Kanoufi, *Chem. Mater.* **2008**, *20*, 6677.
[15] a) C. P. Andrieux, I. Gallardo, J.-M. Savéant, K. S. Su, *J. Am. Chem. Soc.* **1986**, *108*, 638; b) A. Houmam, *Chem. Rev.* **2008**, *108*, 2180.
[16] J.-M. Noël, A. Latus, C. Lagrost, E. Volanschi, P. Hapiot, *J. Am. Chem. Soc.* **2012**, *134*, 2835.
[17] S. R. Wasserman, Y.-T. Tao, G. M. Whitesides, *Langmuir* **1989**, *5*, 1074.
[18] J. Zhang, C. J. Slevin, P. Scott, D. J. Walton, P. R. Unwin, *J. Phys. Chem. B* **2001**, *105*, 11120.
[19] B. Liu, A. J. Bard, M. V. Mirkin, S. E. Creager, *J. Am. Chem. Soc.* **2004**, *126*, 1485.

[20] D. Zigah, C. Herrier, L. Scheres, M. Giesbers, B. Fabre, P. Hapiot, H. Zuilhof, *Angew. Chem.* **2010**, *122*, 3225; *Angew. Chem. Int. Ed.* **2010**, *49*, 3157.
[21] M. Kongsfelt, J. Vinther, K. Malmos, M. Ceccato, K. Torbensen, C. S. Knudsen, K. Gothelf, S. U. Pedersen, K. Daasbjerg, *J. Am. Chem. Soc.* **2011**, *133*, 3788.
[22] F. Grisotto, A. Ghorbal, C. Goyer, J. Charlier, S. Palacin, *Chem. Mater.* **2011**, *23*, 1396.
[23] I. A. Olson, W. A. Bacon, Y. Y. B. Sosa, K. M. Delaney, S. A. Forte, M. A. Guglielmo, A. N. Hill, K. H. Kiesow, R. E. Langenbacher, Y. Xun, R. O. Young, W. J. Bowyer, *J. Phys. Chem. A* **2011**, *115*, 11001.
[24] Y. Guillemin, M. Etienne, E. Sibottier, A. Walcarius, *Chem. Mater.* **2011**, *23*, 5313.

